Journal of the Korean Society of Marine Engineers, Vol.28, No.2, pp.163~184, 2004(ISSN 1226-9549)

Aerothermal Vortex Technologies in Aerospace Engineering

A. A. Khalatov† · Chung-Do Nam*

(Manuscript : Received SEP 18, 2003 ; Revised NOV 28, 2003)

Abstract : Vortex flow fundamentals have been investigating for about hundred years and many distinguished features had been discovered and comprehensively studied over that time. Due to unique hydrodynamic features vortex flows are now widely used in many industrial applications, including energy and power systems, combustion chambers, fuel sprayers, heat exchangers, clean-up systems, drying chambers. Up to recently aerospace engineers employed vortex flow only in combustion systems to stabilize a flame zone or in advanced heat exchangers to enhance heat transfer processes. This paper provides an overview of some recently developed aerothermal vortex technologies applied to aerospace engineering.

Key words : Vortex Flow, Swirl Flow, Turblence, Cyclone Cooling

1. Examples of induced vortices

The vortex flow is a commonly used term to characterize the flow with rotational velocity. In a vortex (cyclone) chamber due to the negligible axial velocity the flow pattern is two-dimensional or quasi two-dimensional, while in-tube decaying swirl flow has comparable axial and tangential components (three-dimensional flow). As a rule, vortex flow provides an increased turbulence enhancing heat and mass transfer processes. Typical examples of induced vortices are: a). Karman vortex street behind a cross flow tube or beyond surface ribbing (Fig.1.a; c); b). trailing and bound vortices (Fig.1.b; d), generated by the wings or winglets; c). in-passage swirl flow and vortex filaments[2] ; d). Dean vortices and Gortler vortices in a curved passage[3] ; e). Taylor vortices in rotating systems[3] ; f). horseshoe vortex and passage vortex over a guide vane end wall[28-31]. Usually these vortices resulted from the hydrodynamic processes, however in some cases they may design deliberately to enhance or to improve aerothermal or combustion processes. Depending on a

† Corresponding Author(Institute of Engineering Thermophysics, National Academy of Sciences, Ukraine-Korea Maritime University)
* Korea Maritime University

situation, the vortex cross size and its length vary from a few millimeters in induced vortices to a couple of miles in the natural tornadoes.

2. Turbine blade cooling

Usually increases in the thermal efficiency of gas turbine cycle can be achieved through higher gas inlet temperatures. In prototype aeroengine gas turbines the entry temperature has already reached 1800K 1900K, while the air ratio in the compressor has gradually approached factor of 45.0. Throughout the gas turbine history developments in heat resistance alloys have lagged behind designers requirements. Since high performance gas turbines operate at gas temperature levels much above the blade melting point, both internal and external cooling systems are widely employed to meet the blade service life requirements.

The Conway (UK) was the world first gas turbine aero-engine with internally cooled blades to enter into service in the year 1962; now the cooling system has become an integral part of all high performance aero-engines. Currently some twenty five heat transfer augmentation techniques are used in various applications. Despite this, till now designers of blade cooling systems employ very limited number of heat transfer techniques, including impingement jets, plain and broken ribs, pin-fins(pedestals), and bulk flow oscillations. The proper combinations of these techniques are used to design modern blade internal cooling systems. However, the thermal

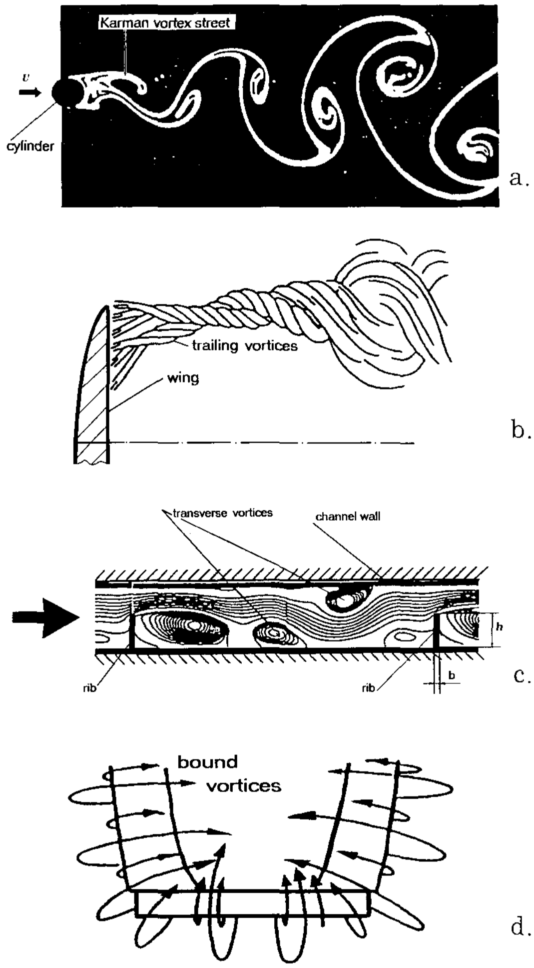

Fig. 1 Examples of induced vortices[48].

a: Karman vortex street behind a circular cylinder in a cross flow.
b: trailing vortices and their tendency in recoil.
c: Karman vortices behind periodic ribs in a channel.
d: equivalent of circulation of bound and trailing vortices.

potential of conventional cooling techniques is nearly exhausted and further improvements in the blade cooling efficiency can be achieved either through increases in a coolant flow rate or by means of reductions in a cooling passage size. Currently there is a *strong demand* for cooling techniques providing high heat transfer without application of small-scale design features difficult in production and prone to dirt blockage problem.

An active research into advanced cooling technologies was initiated recently involving the worldwide leading gas turbine companies, such as General Electric, Pratt & Whitney, Solar Turbines (USA), Rolls Royce (UK) and some leading research centers. The primary requirements to innovative cooling technique are the higher heat transfer rate, lower coolant consumptions, acceptable pressure losses, more simple production technology allowing to avoid manufacture of small size features in cooling systems (passage size; rib height). It seems, the *vortex or swirl flow concepts* addresse actually all these requirements. The most representative examples of the novel technical solutions in gas turbine engineering, based on this concept are considered below.

2.1 Cyclone cooling

Systematic studies of swirl flow were initiated some ninety years ago and many comprehensive books, reviews and journal papers have been published over that time. Despite the comprehensive database [1-3], until recently designers of gas turbine cooling systems did not consider internal swirl flow to be employed in a blade cooling. This is because of conventional cooling techniques enable to secure the required cooling efficiency.

In publications various terms are used to characterize the cooling system employing swirl flow(screw cooling - USA; vortex or cyclone cooling - the former USSR; UK). To avoid misunderstanding the cyclone cooling term is used here to characterise swirl flow in a cooling passage.

The first patent of an airfoil with incorporated cyclone chamber was published in the year 1988[4]. This design is based on a round impingement chamber near the airfoil leading edge and two cyclone chambers in the vicinity of pressure and suction side. In the year 1997 the two-dimensional cyclone chamber for the leading edge area was patented in Ukraine (Fig.2.a; b)[7]. The coolant(air) supplies into a circular-shaped chamber through a single tangential slot to be released onto the blade suction side through few film cooling holes. The vortex with displaced axis of rotation (Fig.2.b) is generated in a cyclone chamber promoting high levels of turbulence and heat transfer, accompanied with permanent boundary layer destructions. In some specific cases related to gas turbine situations, the cyclone cooling effect exceeds effect of the impingement cooling in terms of the average heat transfer rate within an arc 300 (Fig.2.c; d)[16]. The globally averaged heat transfer can be predicted from the correlation:

$$\overline{Nu_D} = 0.190\, Re_D^{\,0.64}, \qquad (1)$$

where $\overline{Nu_D}$ and Re_D is Nusselt and Reynolds number, based on the chamber diameter[9]. The CFD modeling of this configuration has revealed two local heat transfer maximums reflecting the double impingement effect[9].

The quasi two-dimensional cyclone cooling design, based on the spanwise displacement of inlet and outlet tangential slots has been suggested and comprehensively studied in[5]. This design promotes favorable conditions to generate the powerful vortex structure permanently destroying the wall boundary layer. The partitions between separate cooling chambers provide the additional ribbing effect by means of the heat conductivity from the leading edge area.

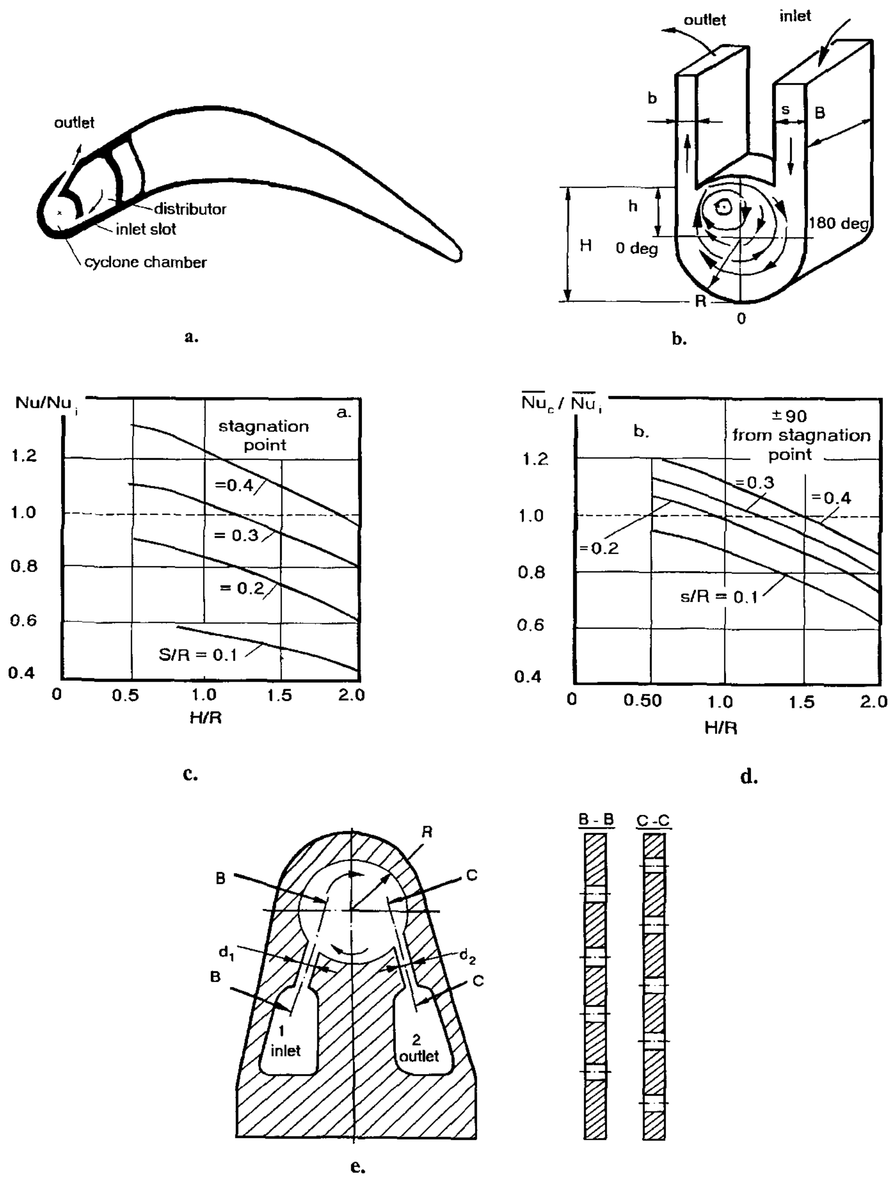

Fig. 2 Two-dimensional and quasi two-dimensional cyclone cooling configurations.
a, b: 2-D cyclone cooling scheme[7]. c, d: results of 2-D scheme testing[16].
e: quasi 2-D cyclone cooling[17].

The cyclone-jet configuration (Fig.2.e) provides a quasi two-dimensional swirl flow pattern in a cooling chamber. Detailed studies have demonstrated this design has a few advantages over the tangential slot scheme (Fig.2.a; b) and the reasonably high Nusselt number ratio (factor of 2.6 - 3.5)[17]. The non-equivalent number of inlet and outlet holes forms the non-uniform heat transfer pattern in the spanwise and angular directions. The angular distribution has a non-symmetrical shape with respect to the chamber stagnation point. Depending on the boundary conditions this distribution has either a flat shape or a sharp maximum at the stagnation point. As found, the globally averaged heat transfer within the chamber is well described by the correlation[17]:

$$\overline{N}u_D = 0.020\ Re_D^{0.8}(d/s)^{0.2}(A_{in}/A)^{-0.1}(T_w/T_{in})^{0.55} \quad (2)$$

Here d, and s is the chamber diameter and height of equivalent inlet slot; A_{in}, and A is the inlet slot and cooling chamber cross section area; T_w, and T_{in} is the average wall temperature and flow inlet temperature.

Some recent results of heat transfer and hydrodynamics measurements in a passage with tangential inlet and outlet are given by Ligrani et al.[10].

The serpentine cyclone cooling design where an air moves successively through three passages and two swirl generators (Fig.3) was tested by Khalatov et al.[12]. The simplified blade with incorporated cooling system is shown in Fig.3.b. The experimental data have demonstrated the high heat transfer rate in both passages (up to a factor of 5.0) at acceptable pressure drop factor (Fig.4). The CFD modeling undertaken in[39] has revealed separation zones in the vicinity of tangential swirl generators causing extra pressure losses. Recently Cheng Quian et al.[11] have concluded the serpentine cyclone configuration can effectively be used in cooling of blade trailing edge area. Results of their conceptual studies have confirmed the swirl flow cooling and impingement cooling have the equivalent heat transfer rate over tangential slot area, whereas within a zone of -2.5 < x/d

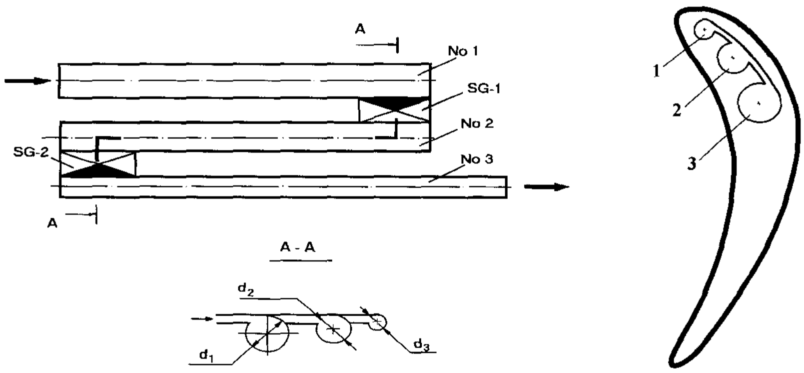

Fig. 3 Serpentine cyclone cooling[12] : flow scheme (a) and blade design (b).
SG-1; SG-2; tangential swirl generators.

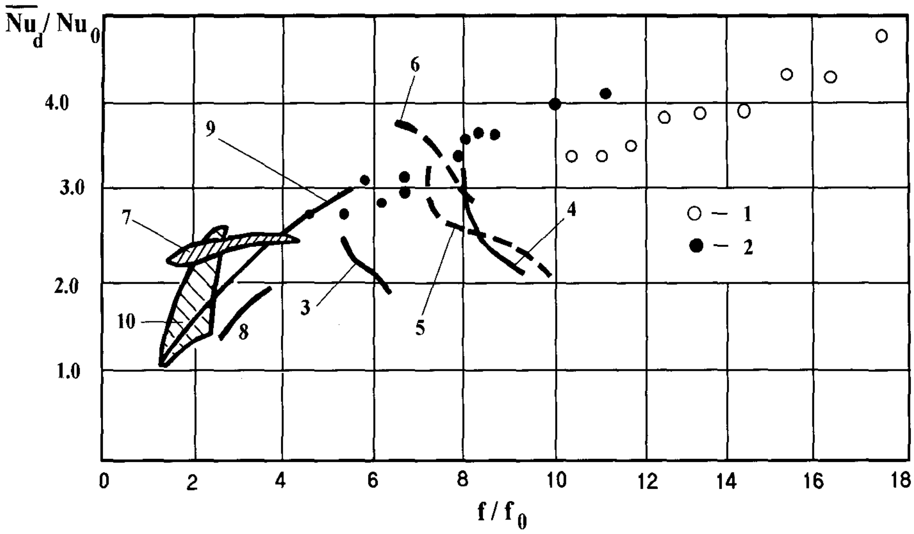

Fig. 4 Serpentine cyclone cooling: thermal-hydraulic performance[12].
1: passage No 2 (Fig. 3). 2: passage No 3 (Fig.3). 3-6: continuous and broken ribs (60 &90 degrees)[21]. 7: surface dimples[21]. 8: pin-fins (pedestals)[16]. 9: vortex matrix[16]. 10: surface dimples[16].

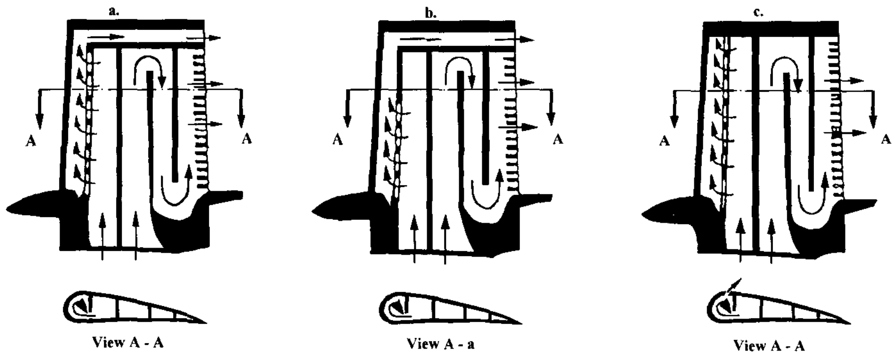

Fig. 5 Three-dimensional cyclone cooling[6].

〈 2.5 the globally averaged heat transfer for a cyclone cooling exceed by 20% the impingement cooling data.

The concept of three-dimensional cyclone cooling (Fig.5) has been suggested and studied by Glezer et al.[6]. This two-passage design is based on a row of tangential slots evenly distributed along a blade span. A coolant discharges either into the trailing edge area (configurations *a* and *b*) or through film holes onto the blade suction side (configuration *c*). Results of heat transfer studies presented in Fig.6 have demonstrated a superior rate of a globally average heat transfer compared with an impingement cooling, trip strips technology and a surface ribbing. The basic advantages have been achieved when a coolant cross-flow occurs along the leading edge area.

Panula et al.[14] have studied the swirl flow design consisting of two rectangular passages separated by a dividing plate. It has been found that crossflow induced swirl associated with an impingement effect provides very high heat transfer level locally reaching factor of 8.0. However, very high penalty in terms of pressure drop have to be paid instead.

Some specific hydrodynamic features promoting enhanced heat transfer in a three-dimensional configuration have been considered by Khalatov[2], Cheng Quian et al.[11], Ligrani et al.[10].

Figure 7 represents the globally averaged Nusselt number as dependent upon Reynolds number for various cyclone cooling configurations. Both dimensionalless numbers are based on a chamber diameter so that to summarize the published data. The experimental data, describing both 2-D configuration and quasi 2-D configuration are well

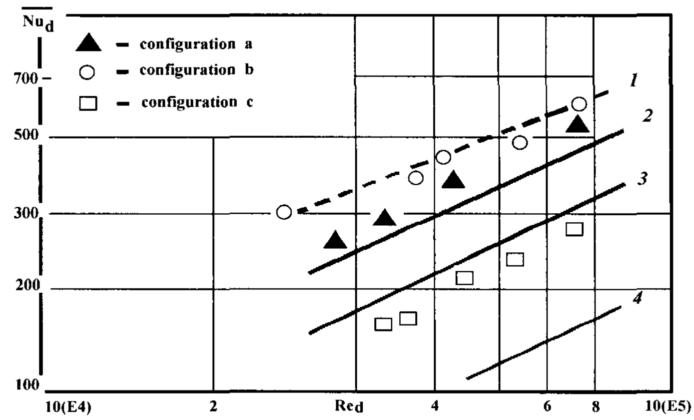

Fig. 6 Three-dimensional cyclone cooling[6] : results of testing and comparisons[9]

1: impingement cooling with film cooling. 2: impingement cooling with cross-flow. 3: trip-strips technology. 4: smooth passage.

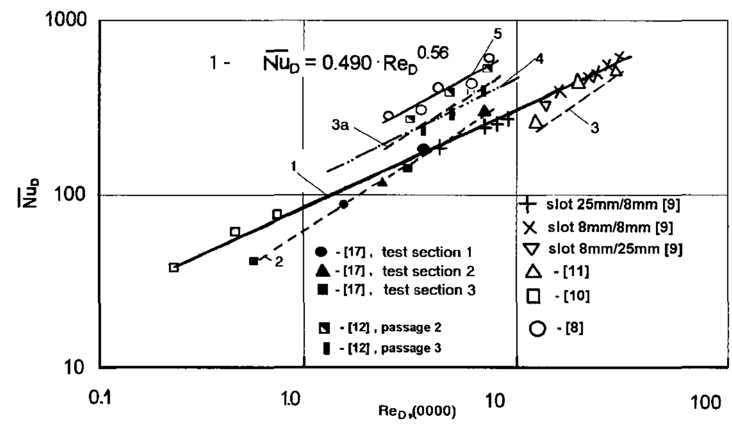

Fig. 7 Summarizing of published data.

represented using an equation of the form:

$$\overline{Nu_D} = 0.490\ Re_D^{0.56} \quad (3)$$

This correlation is valid for a wide range of Reynolds number from 2,000 to 300,000. Only the limited data of the test section number 3[17] have a tendency to diverge from the correlation (3) at low Reynolds numbers (ReD < 16,000). The correlation (3) exceeds data of an impingement cooling (curve 3;[11]); the results for three-dimensional configurations (curve 4 [23]; curve 5 [8];[12]) exceed 2-D and quasi 2-D data. The curve 3.a indicates the impingement cooling data at a cross-flow [8].

All published papers, available and recently registered patents [51-53] demonstrate a great potential of the swirl flow concept to be applied in design of advanced blade cooling systems. The higher heat transfer rate is able to extend the temperature limit of internal cooling system. There has been reported [8] that extension from 1176℃ turbine entry temperature to 1260℃ can be achieved if the two-passage cyclone cooling design (Fig.5.a) applies instead of conventional ribbed cooling. It seems, substantial benefits from the swirl flow application can be obtained in gas turbine situations when increase in pressure losses brings no the cycle penalty problem (insufficient flow filling in cooling passages).

In addition to the higher heat transfer rate, the swirl flow concept has some other attractive features. Since the centrifugal effect squeezes a hot air into internal passage area, the constant coolant refreshment effect is occurred in a cooling passage. Due to a high static pressure on a passage wall some improvements in an external film cooling can also be expected. A blade rotation does not destroy the cyclone cooling efficiency [13], unlike other cooling techniques the elements of a cyclone cooling fully assimilate the centrifugal load. The most distinguishing feature of a cyclone cooling is the ability to simplify production technology and to avoid manufacture of small size features prone to dirt blockage problem (ribs typically of 0.4 mm in height; passages smaller than 1 mm in a diameter). Swirl flow concept cause some extra pressure losses, however design compromises can be accepted if the high heat transfer rate and acceptable thermal-hydraulic performance are optimized with the cost effective technology.

2.2 Vortex matrix

The vortex matrix (lattice cooling [19]) represents two sets of inclined, repeated, parallel ribs and channels (Fig.8.a). After connection this forms small rectangular-shaped passages intersecting under the angle 2β and closed at lateral sides. The top of ribs is in a tight contact and flow can communicate between channels.

From the inlet to lateral side a coolant moves as an axial flow both within the top and bottom passages. At the right side the bottom coolant is transferred up to the top channels, whereas at the left side it moves downwards the bottom passages (Fig.8.a). Due to the vortex impingement each flow turn (Fig.8.b) acts as a local swirl generator and creates the swirl flow pattern in each rectangular-shaped passage (Fig.8.c).

Each in-passage swirl flow is not decaying: communication between upper and lower flows and exchange of rotational momentum (Fig.8.d) provides an approximately permanent swirl flow rate in the downstream direction. Results of numerical modeling given in [18] have confirmed the above swirl flow pattern in the rectangular passage.

Four plain vortex packages with ribs inclined to one another at 30, 60, 90 and 120 degrees have been tested in [42] for stationary conditions. The Nusselt ratio normalized by the Dittus-Boelter correlation (Nu_{av} is a globally averaged Nusselt number) is approximately constant throughout the package to be varied from 1.2 to 1.9 in the range of Reynolds numbers tested. At the given pressure ratio $P_{total\ in}/P_{static\ out}$ the greatest heat transfer enhancement was registered at 90 degrees (Fig.9). The maximum local heat transfer coefficient h_m was registered at around 15-20 degrees beyond the stagnation point (Fig.8.b). Actually, the same qualitative results were obtained in [16] where the maximum Nusselt ratio achieved was about 2.9.

The blade design entirely using the vortex matrix is shown in Fig.10. The highest average cooling effect was registered on the blade suction side, whereas the lowest one was found at the

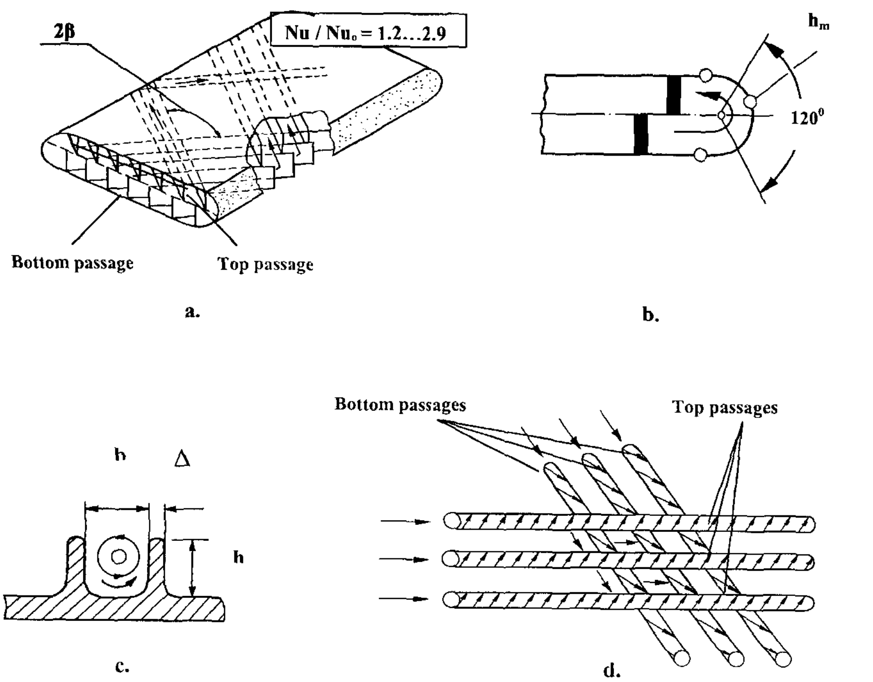

Fig. 8 Plain vortex matrix.
a: plain package. b: swirl flow turn. c: in-passage swirl flow. d: swirl flow pattern.

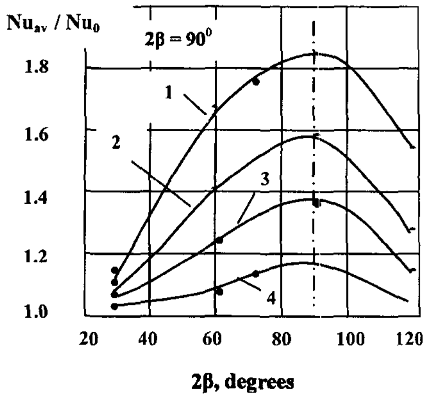

Fig. 9 Heat transfer in a vortex package [42].
Re : 1 - 2500. 2 - 5000. 3 10000. 4 20000.

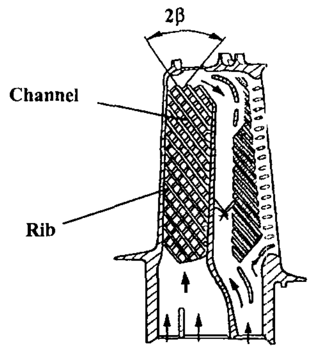

Fig. 10 Blade with incorporated vortex matrix [42].

blade stagnation point [42]. If the pressure ratio increases, then the blade cooling efficiency increases too; the globally averaged heat transfer is approximately the same as the average heat transfer found on the blade pressure side. Introduction of film cooling in the leading edge area increases the blade cooling efficiency at the constant pressure ratio $P_{total\ in}/P_{static\ out}$ due to a higher mass flow coming through the blade.

Along with improved heat transfer efficiency the vortex matrix concept offers designer a higher structural integrity. The integral casting of both sets of channels produces a very strong blade as the faces arc tied together. This could allow the use of thinner blade walls than in conventional cooling designs. This benefit may be out weighed by the increased weight of the blade and localized root stresses. The vast experience gained in the former USSR [16, 42] has demonstrated improved life of the rotating blade with incorporated vortex matrix. As shown [16], the thermo cyclic strength (number of cycles to failure) of the blade with a vortex matrix is up to one hundred times greater than that occurring for the trailing edge supplied with pin-fin technique. However, recent investigations undertaken jointly by Rolls Royce (UK) and Oxford University (UK) have revealed insufficient heat transfer uniformity in the trailing edge area [19].

2.3 Surface dimple technique

The surface dimple technique is based on formation of in-dimple oscillating vortex bursting periodically into a freestream flow. Results obtained in the former USSR and then in USA have demonstrated the reasonably high heat transfer rate accompanied with approximately equivalent pressure drop factor [20, 22, 23].

One of the earliest studies of a flow pattern near dimpled balls were undertaken in [43]. As seen (Fig. 11), at Re $<$ 2×10^5 the drug coefficient of the dimpled ball is substantially lower than that over a smooth ball.

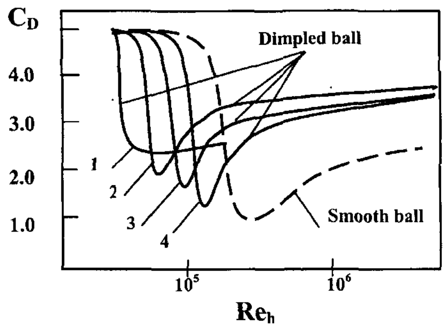

Fig. 11 Drug coefficient of dimpled balls [43].

In a shallow dimple (h/D < 0.1 - 0.2) made on a flat plate the flow is usually without separation. Within a deep dimple (h/D > 0.2) a pair of vortices is formed at the trailing edge area moving towards the leading edge (Fig.12). The in-dimple backflow velocity is around 40% from the freestream velocity [22]. At the dimple pole these vortices are united together to create the inclined single vortex, bursting periodically into the downstream flow. The vortex pole is not a stable, but oscillates within the angle of ±45 degrees (Fig.13). The frequency of the angle oscillations and the vortex-from-dimple bursting depends upon the Reynolds number, freestream turbulence, and channel geometry. The mechanism of the vortex-in-main flow breakdown is very unique (dissipation of ring vortices), that provides markedly reduced pressure losses. Unlike a single dimple the family of surface dimples on a flat plate promotes an interaction of separate vortices creating the gang of vortices [20, 23, 25, 50].

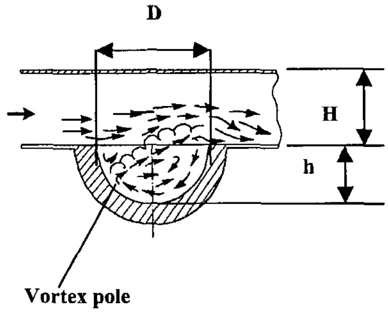

Fig. 12 In-dimple flow pattern.

Precise measurements and flow observations have revealed the tornado-like nature of the oscillating vortex with concentration of rotation momentum near the vortex axis. Local heat transfer coefficients between dimples are given in Fig. 14; the overall heat transfer ratio reaches factor of 2.2 - 2.7 in a wide range of boundary conditions (dimples on one and both channels sides) [16, 21, 23]. This accompanies with approximately equivalent pressure drop factor [16, 21, 23, 25, 26]. The heat transfer rate increases at the growth of f parameter and reductions in h/D ratio; the pressure drop decreases at a growing of f and Δ/D numbers (maximum at h/D 0.5). Here $f = (\pi D^2/4) / (t_x t_z)$ is the density of dimples; H is a channel height; D and h is the dimple diameter and depth; t_x and t_z are the dimple pitches in the streamwise and spanwise direction. No effect of the channel height was found on the heat transfer rate and pressure drop factor in a dimpled channel [16, 23]. At a cross flow of dimpled tubes the heat transfer increases by 20%, while the pressure drop factor reduces by 20% - 50% compared with bundle of smooth tubes. The displacement of separation point

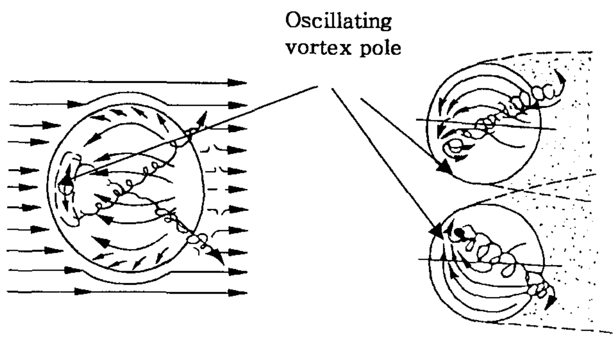

a.

Fig. 13 Schematic of in-dimple flow phenomenon.

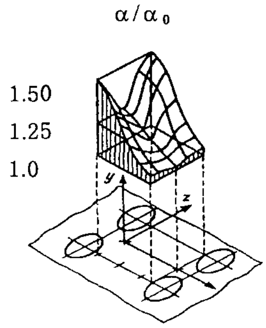

b.

Fig. 14 Local heat transfer diagram [47].

towards the rear tube area and reductions in pressure drop were registered at the air cross flow of a single dimpled tube.

Limited publications are concerned with effects of boundary conditions, such as a streamwise pressure gradient and freestream turbulence [47]. Recent investigations have demonstrated remarkable role of a surface curvature on heat transfer within a dimple [24, 50]. The factor of 3.9 was reached in a single dimple arranged on a concave wall against the factor of 2.2 - 2.5 observed on a smooth flat plate at identical flow conditions [24]. The effect of dimpled surface on a local heat transfer for multiple jet impingement has been reported in [44]. As found, Nusselt numbers for a dimpled and smooth surface are about the same, however the dimpled surface provides higher heat transfer due to increased surface area when compared with a smooth surface.

Experiments performed in [16] have shown that turbine blade supplied with internally protruded dimples keeps the centrifugal load ability in the range of f 〉 70% and h/D 0.13, provided that blade cross-section area is identical to that occurring before dimpling. Dimples arranged on the inner surface of pressure and suction side, as well as in the trailing edge area increase the blade service life by factor of 2.0 - 3.0 when compared with blade having smooth cooling passages [16].

The bulk of published results are concerned with a dimpled flat plate. In situations where a surface geometry is close to a flat configuration these results have been used for a cooling of combustor lines, coolant-to-blade supplying channels, back surface of a guide vane end wall. The unique properties of the bursting vortex have led to the idea of oscillating film cooling, where a coolant supplies to the dimple 'pole' area (Fig.13.b) to be introduced into the vortex axis. Flow visualizations by means of a fine powder blowing have shown [22] a powder is effectively sucked into the vortex center to cover a wider wake area beyond a dimple. This provides better film cooling

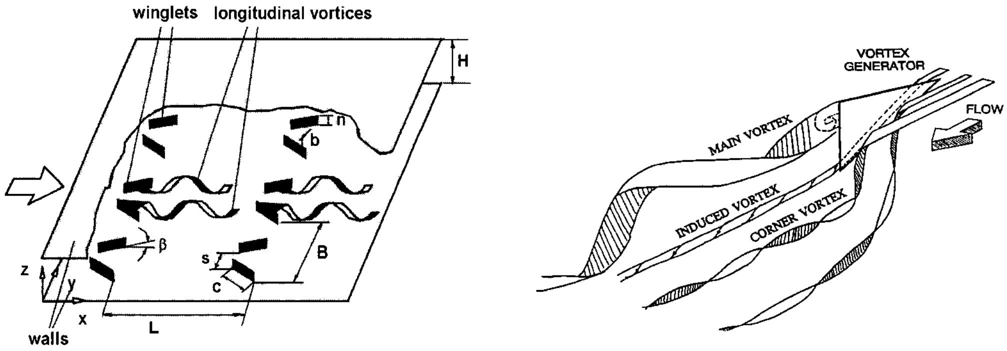

a. b.

Fig. 15 Induced longitudinal vortices [48].

a: array of rectangular winglets. b: vortex system, generated by a half-delta wing.

coverage and, as a result the better film cooling effectiveness.

The engraving of dimples into the blade suction surface of the low-pressure aero engine gas turbine leads to reduction in flow separation losses at all Reynolds numbers and turbulence intensities [45]. This improves engine efficiency during the high altitude loiter phase. Recent investigations [46] have demonstrated that surface dimples can effectively be used in combustion processes. Combustion process destroys the twin vortex inside a dimple and transforms it into the toroid-shaped vortex structures. A stable burning of the natural gas within a hemispherical dimple is observed when the gaseous fuel supplies closer to the dimple trailing edge area.

3. Surface vortex generators

The surface vortex generators are protrusions from a heat transfer surface, which are designed to generate vortices spiral around their axis in the streamwise direction. The trailing vortices behind the rectangular winglets (Fig.15), half-delta, and delta wings are classical examples of longitudinal vortices. Besides the main vortices shown in Fig.15, a horseshoe vortex or corner vortex develops in the stagnation region of the vortex generator. A Karman vortex street (Fig.1.a) may also develop beyond the trailing edge of the vortex generator. The details of the vortex system are strongly influenced by the geometry and Reynolds number. Rectangular winglets, wings and delta wings can easily be incorporated into the heat transfer surfaces (boundary layer: channels) by stamping, embossing or attachment.

Detailed review of heat transfer and hydrodynamics was reported by Fiebig [48]. The longitudinal vortices enhance heat transfer both locally and globally in their corkscrew motion and are very persistent both in laminar and turbulent flows. However, heat transfer enhancement is higher in laminar flow. Winglets cause higher heat transfer enhancement than delta wings for identical conditions, triangular and rectangular winglets give approximately similar performance if all other dimensionless parameters are the same. Global heat transfer enhancement of more than 100% over 40 times the vortex generator area were achieved for a single row of delta winglets [48].

Detailed measurements of local Nusselt number distributions and surface friction in a square duct with twelve different vortex generators were presented in the comprehensive paper [49]. The best vortex generators were identified in terms of a heat transfer augmentation and uniformity, as well as pressure drop factor. As a whole, the potential of vortex generators for heat transfer control is very high because of the generated heat transfer mechanisms and the possible variations.

4. Thermal-hydraulic performance

The diagram of thermal-hydraulic performance for actually all heat transfer techniques is presented in Fig. 16. It includes conventional cooling techniques applied in gas turbine engineering, vortex technologies, as well as heat transfer techniques employed in various applications. The *a-curve* is the Reynolds analogy line; the *b-b* area comprises of the surface roughness effect. The following *primary conclusions* can be drawn from this diagram analysis.

4.1. Three passage serpentine cyclone cooling (21) and an in-tube decaying swirl flow (17) exceed all other

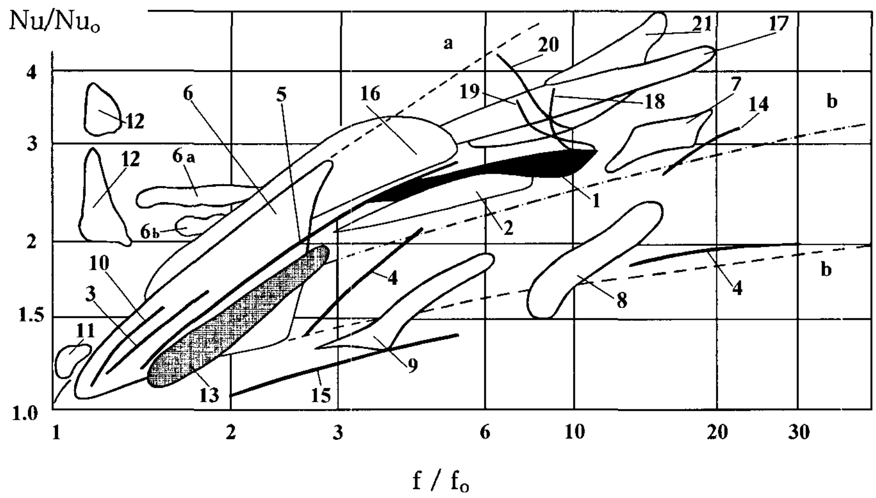

Fig. 16 Diagram of thermal-hydraulic performance.

a: Reynolds analogy line. *b-b*: area of a surface roughness effect.
1: internal annular ribbing. 2: hemispherical surface bulges. 3: twisted tape inserts. 4: pin-fins (pedestals). 5: vortex matrix [16]. 6: hemispherical surface dimples [16]. 6.a: hemispherical surface dimples [21]. 6.b: hemispherical surface dimples [23]. 7: internal spiral grooves. 8: hemispherical bulges-dimples. 9: internal grooves. 10: warm pipes. 11: small rib lets. 12: hemispherical surface bulges (boiling). 13: channels of variable cross-section. 14: zigzag channels.
15: curved channels. 16: oval twisted tubes. 17: in-tube swirl flow. 18: 90 degrees broken ribs [21]. 19, 20: 60 degrees continuous and broken ribs [21]. 21: three passage serpentine cyclone cooling (Fig. 3) [12].

techniques in terms of the heat transfer ratio at a fixed pressure drop factor. Both techniques also exceed results obtained for advanced continuous and broken ribs (18-20). The oval twisted tubes data (16), providing continuous flow swirl are scattered around the Reynolds analogy line.

4.2. Vortex matrix data (5) scatter within a fairly narrow zone, but they cover a broad area of the Nusselt ratio from 1.2 to 2.9. The best results are as good as an internal annular ribbing widely used in advance thermal systems.

4.3. Surface dimple data (6) cover a broad area of Nusselt ratio. The best design in terms of the maximum heat transfer rate (Nu/Nu_0) was found at f = 67%; h/D 0.13 and $H/D < 0.17$ [16]. Recent experiments carried out in USA (6a; 6b) are located over the roughness effect area b-b and the bulk of them exceed the Reynolds analogy line. Unlike data of [16], these results do not depend upon the pressure drop factor.

Both semispherical surface bulges technique (2) and bulges-dimples technique (8) are comparable with surface dimples in terms of the heat transfer level, however they suffer from increased pressure penalties. The surface dimple technique being above the Reynolds analogy line cannot be qualified as a pure surface roughness technique. Obviously, it is due to unique mechanism of the vortex breakdown in the mainstream flow.

5. Guide vane end wall

Continuous elevations in the turbine inlet temperature, increases in the compressor air pressure ratio and heat loading in turbine stage have led to reductions in the blade height-to-pitch ratio and growth of flow turn angle within a blade passage.

The end wall flow pattern (Fig.17) includes a cross flow from the pressure to suction side, as well as vortex flow in form of a horseshoe vortex formed in front of a leading edge, passage vortex

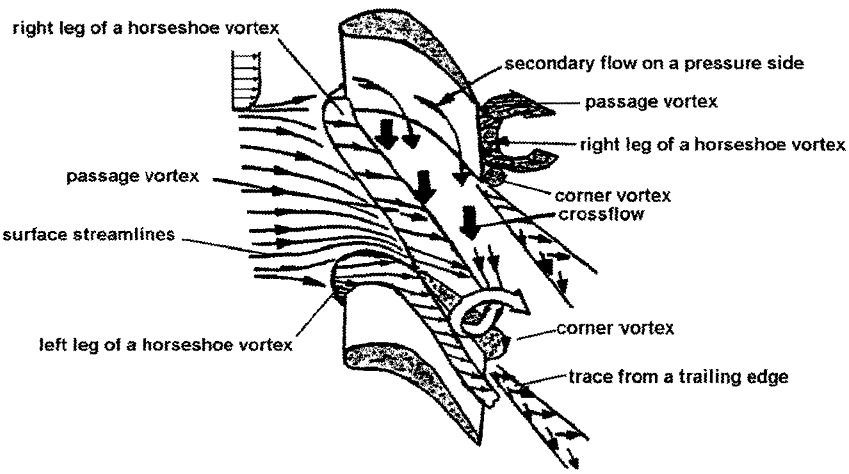

Fig. 17 End wall flow pattern [33].

moving across the end wall, and a cluster of small but intense corner vortices. The resulted three-dimensional flow pattern provides a complex end wall heat transfer distribution. The average heat transfer enhancement effect is within factor of 1.3 - 1.5 compared with flat plate data at identical Reynolds numbers [33], whereas local increases can achieve factor of 3.0. The passage vortex lifted onto the blade suction side brings additional pressure losses and blade cooling problems. Since these vortices bring extra heat transfer effect, their effect should be minimized as much as possible.

Many researches into the secondary flow and heat transfer patterns were carried out over the last two decades. It was concluded these flows have substantial impact on the heat transfer and film cooling efficiency throughout the end wall area. Detailed heat transfer reviews have been given by Harvey and Jones [27], Khalatov [28]. Wang et al. [29] has summarized three representative flow pattern models described in the literature. Some important flow details have been reported by Goldstein and Spores [30], Chung and Simon [31], Jabbari et al. [32], and some other investigators.

The Institute of Engineering Thermophysics (Kiev, Ukraine) was involved in many research programs of the former USSR aimed at improvements in end wall cooling. These studies include the following primary subjects:

- Novel approach at the end wall heat transfer analysis [33], based on the isolated effects of streamwise and spanwise pressure gradients; boundary layer three-dimensionality; vortex structures; free stream turbulence; coolant blowing through a permeable end wall.

- Heat transfer over a smooth end wall, including effect of free stream turbulence [34].

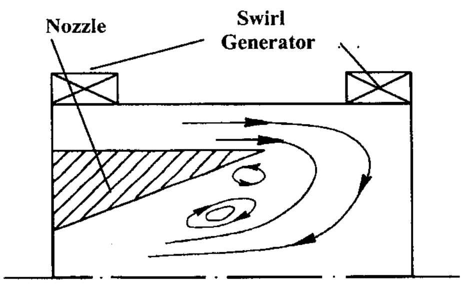

a.

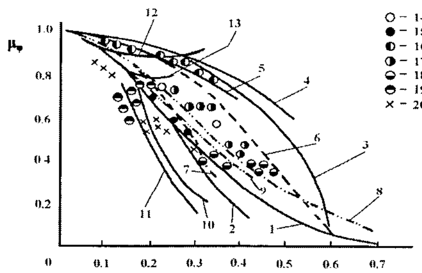

b.

Fig. 18 Nozzle with flow swirl [3].

a: nozzle with two tangential swirl generators. *b*: discharge coefficient: nozzle with flow swirl. 113: *Predictions*. 1, 2: free vortex rotation. 3, 4: solid body rotation. 5: corkscrew flow model. 6, 7: compound law: solid body and free vortex rotation. 8, 9: exponential law. 10, 11: free vortex rotation (rotating flow predominance near a nozzle axis). 12, 13: free vortex rotation (axial flow predominance near a nozzle axis). 14-20: *Experiments*. 14: blade swirl generator. 15: tangential swirl generator (pre-nozzle tube l/d = 1.5). 16: tangential swirl generator (pre-nozzle tube l/d = 0). 17, 18: tangential swirl generator (pre-nozzle tube l/d = 1.5-3.0; 1.0). 19, 20: tangential swirl generator (pre-nozzle tube l/d = 1.0; Inlet = 1500K).

- Heat transfer over a permeable end wall, including effect of freestream turbulence [35].

- The upstream or downstream secondary flow near a blade suction or pressure side; interaction of passage vortex with blade suction side; associated heat transfer and pressure losses.

Some other results obtained in the former USSR and unknown in the West include pre-end wall film cooling; compound pre-end wall film cooling; discrete holes spread over the end wall area; supersonic end wall heat transfer. The novel technique of end wall contouring aimed at preventing of vortex flow has been studied by many authors, including Hartland et al. [36], Yan et al. [37], Simon et al. [38].

6. Nozzle with inlet flow swirl

The axial and rotational velocities of swirl flow are very complex in a shape [1, 2], providing reductions in the passage discharge coefficient. This particular feature was used in developing of small size supersonic nozzle (Fig.18.a) enabling to vary the nozzle thrust by a few times at the fixed mass flow. Depending on the swirl flow ratio α^* [3] and rotational velocity profile the discharge coefficient vary in a wide range (Fig.18.b); these reductions can be achieved either through increases in the swirl flow ratio or via variations in the rotating velocity profile at the constant swirl flow ratio. The following basic conclusions can be drawn *from the data presented in Fig. 18.b.*

- Free vortex rotation with predominance of rotating flow at a nozzle axis provides the most significant influence on the discharge *coefficient* (curves 10, 11), while the solid body rotation has a minimum effect (curve 4). Both the compound law (curves 6, 7) and exponential law data (curves 8, 9) lie between them.

- Corkα^* < 0.3.screw flow model (curve 5) and flow solid body rotation give approximately the same results at

- Tangentiaα^* < 0.3 - 0.45 are well agreed with the corkscrew model and compound law (*solid body rotation up to* r / R = 0.9).l flow swirl at the nozzle inlet: the experimental data for

- At α^* = 0.08 - 0.17 there is a significant scattering of experimental data. Obviously, at α^*= const the flow changes its structure from one type of a flow predominance (curves 10, 11) to another (curves 12, 13).

When the flow rotation is generated at the nozzle inlet ($l/d_{in} = 0$) the *experimental data are well described by* the correlation:

$$\mu_\varphi = \exp(-0.78\,\alpha^*) \tag{4}$$

If the length of pre-nozzle passage is l/din < 3.0, the discharge coefficients are lower of those predicted from the equation (4) and are described by the correlation:

$$\mu_\varphi = \exp(-1.8\,\alpha^*) \tag{5}$$

The latter is well agreed with the free vortex rotation model (curve 1), suggested by Mager [2, 3].

7. Conclusions

Vortex aerothermal technologies have a great potential to be applied to gas turbine engineering in advanced cooling systems; small size supersonic nozzles; components of aeroengines. They have a reasonably high heat transfer at acceptable pressure losses.

- Blade cyclone cooling is able to achieve very high heat transfer ratio (factor of 6.0 8.0) at acceptable thermal-hydraulic performance. This technology enables avoiding of very small features manufacturing in cooling passages (ribs smaller than 0.4 mm; passages smaller than 1mm in a diameter). Cyclone cooling elements fully assimilate the centrifugal loading in rotating blades.
- Surface dimple technique demonstrates the record thermal-hydraulic performance associated with a simple production technology. Along with a blade cooling, recent applications include combustion processes and flow separation control in the low-pressure aeroengine gas turbines.
- Vortex matrix reveals the high heat transfer rate associated with increased blade operating longevity. The higher structural integrity (full assimilation of the centrifugal loading) produces a very strong blade allowing to cast thinner blade walls than in conventional cooling designs. This benefit may be out weighed by the increased weight of the blade and localized root stresses.
- Vortex flow has substantial impact on heat transfer over a guide vane end wall. Some novel approaches have been developed and studied (end wall contouring) to prevent the vortex flow effect on convective heat transfer.
- Swirl flow features provide favorable conditions to range widely the small-size supersonic nozzle thrust at the constant mass flow rate.

8. Acknowledgements

This research has been sponsored partly by the NATO Scientific Committee (Belgium) under a Collaborative Linkage Grant SA (PST. CLG.976807) 5732.

9. References

[1] Gupta A.K., Lilley D.G., & Syred N. Swirl Flows. Abacus Press, Tunbridge Wells (Publishers), England, 1984.

[2] Khalatov A.A. Swirl Flow: Fundamentals and Applications. Ukraine, Naukova

[3] Khalatov A.A., Avramenko A.A. & Shevchuk I.V. Heat Transfer and Hydrodynamics in Centrifugal Fields. *Vol. 1*: Curved Flows and Surfaces (1996); *Vol. 2*: Rotating Systems (1996); *Vol. 3*: Swirl Flows (2000), *Vol. 4:* Industrial Applications (2000). The National Academy of Sciences of Ukraine (Publishers), Kiev, Ukraine (in Russian).

[4] Smith, N. Cooled Compound Elements of Airfoil. Patent of UK, No 2202907, 10.01.88, 416/96 R.

[5] Varganov I. S., Khalatov A. A. & M. Mitrakhovich M. M. Cooled Blade of Guide Vane. Patent of Ukraine No 10515A, 25.12.96., Priority of 05.12.94.

[6] Glezer B., Tsuhon Lin, & Moon

Hee-Ko. Turbine Cooling System. Patent of USA, No 5,603,606, February 1997, 416/97 R; 415/115, Priority of November 1994.

[7] Geletuha G. G. & Khalatov A. A. Jet-cooled Cyclone System. Patent of Ukraine, No 20116A, 25.12.97, Priority of 05.12.94.

[8] Glezer B., Moon H.K., & OConnel T. Novel Technique for Internal Blade Cooling. *ASME Paper 96-GT-181, 1996.*

[9] R. M. AL-Ajmi, Syred N., Bowen P., & Khalatov A.A. Evaluation of Vortex Cooling System for Turbine Blades. *Proceedings. of FEDSM98, 1998 ASME Fluids Engineering Division Summer Meeting, FEDSM98-4996*, June 21-25 1998.

[10] Ligrani P.M., et al. Flow Phenomena in Swirl Chambers. *ASME Paper 97-GT-530, 1997.*

[11] Cheng Kian et al. Innovative Vortex Cooling Concept and its Application to Turbine Airfoil Trailing Edge Cooling Design. *The 33d AIAA/ ASME/SAE/ASEE-Conference, Paper 97-3013, 1997.*Flow Within Double Overlapped Passages. Report No 2624, 2000, Cardiff University, United Kingdom.

[12] Khalatov A. A., Syred N., Bowen P., et al. Innovative Cyclone Cooling Scheme for Gas Turbine Blade: Thermal-Hydraulic Performance Evaluation. *ASME Paper2000-GT-237.* The 2000 International Joint Power Generation Conference and Exposition, May 8-11, 2000, Munich, Germany. *ASME Paper 2000-GT-230, 2000.*

[13] Glezer B., et al. Heat Transfer in Rotating Radial Channel With Swirling Internal Flow. *ASME Paper 98-GT-214, 1998.*

[14] Panula, G., Ekkad, S., & Acharya, S. Influence of Cross-flow Induced Swirl and Impingement on Heat Transfer in a Two-pass Channel Connected by Two Rows of Holes. *ASME Paper 2000-GT-230.* The 2000 International Joint Power Generation Conference and Exposition, May 8-11, 2000, Munich, Germany.

[15] Kopelev, et al., Heat Transfer Studies: Development of Gas Turbine Cooling Systems. *Izvestiya Academii Nauk, Energetika i Transopt,* No 3, 1989 (in Russian).

[16] Nagoga, G. P., Effective Blade Cooling Techniques for High Performance Gas Turbines. Moscow Aviation Institute (Publishers), Moscow, 1996 (in Russian).

[17] Khalatov. A. A., Syred N., Bowen P. G., $ Al-Ajmi R. Quasi Two-Dimensional Cyclone-Jet Cooling Configuration: Evaluation of Heat Transfer and Pressure Losses. The 2001 International Joint Power Generation Conference and Exposition. June 4-7, 2001, New Orleans, USA. *ASME Paper 2000-GT- 230*, ***2000.***

[18] Smith, A. & Khalatov, A. A. CFD Study Into the Hydrodynamics and Patterns of Three-Dimensional Swirling Dumka, National Academy of Sciences of Ukraine (Publishers), 1989 (in Russian).

[19] Gillespie, D. R., Ireland, P., &

Dailey, G. M. Detailed Flow and Heat Transfer Coefficient Measurements in a Model of an Internal Cooling Geometry Employing Orthogonal Intersecting Channels. *ASME Paper 2000-GT-653*, 2000.

[20] Gachechiladze, A. et al., Heat Transfer at Self-Formation of a Whirlwind Structure, *Heat/Mass Transfer. Convective, Problem Reports: Radiation and Complex Heat Transfer*, Minsk, ITMO AN BSSR, 1988, pp.83-125 (in Russian).

[21] Chyu, M.K., Yu,.Y., Ding, H. Downs, J.P., & Soechting, F.O., Concavity Enhanced Heat Transfer in an Internal Cooling Passage, *ASME Paper 97-GT-437, 1997.*

[22] Kesarev, V.S. and Kozlov, A.P., Flow Pattern and Heat Transfer Over a Hemispherical Dimple Flowed by Turbulized Airstream, *Vestnik MGTU, Ser. Mashinostrostroenie*, No., pp.106-115 (in Russian).

[23] Moon, H. K., OKonnel, T., and Glezer, B., Channel Height Effect on Heat Transfer and Friction in a Dimpled Passage, *ASME Paper 99-GT-163, 1999.*

[24] Khalatov, A. A., Syred, N., et al., Effect of a Surface Curvature on Heat Transfer and Hydrodynamics Within a Single Hemispherical Dimple, *ASME Paper 2000-GT-236, 2000.*

[25] Mahmood, G. I., Hill, M. L., Nelson, D. L., and Ligrani, P. Local Heat Transfer and flow Structure on and Above a Dimpled Surface in a Channel. *ASME Paper 2001-GT-230, 2001.*

[26] Gortyshov, Yu. F., Popov, I. A., Amirhanov, R. D., & Gulitsky, K.E. Studies of Hydrodynamics and Heat Exchange in Channels with Various Types of Intensifiers. Heat Transfer 98, Proceedings of 11th IHTC, Vol, 6, August 23-28, 1998, Kyongju, Korea.

[27] Harvey, N. W., and Jones, T.V., Measurements and Calculations of End Wall Heat Transfer and Aerodynamics on a Nozzle Guide Vane in Annular Cascade, *ASME Paper 90-GT-301, 1990.*

[28] Khalatov, A. A., Heat Transfer and Hydrodynamics on the End Wall of a Gas Turbine Cascade Nozzle with Intensive Secondary and Vortex Flows, *Promyshlennaya Teplotkhnika*, 1993, Vol. 15, No 4, pp.3-18 (in Russian).

[29] Hai-Ping Wang, Olson, S. J., Goldstein, R. J., & Eckert R. G., Flow Visualisation in a Linear Turbine Cascade of High Performance Turbine Blades, *ASME Paper 95-GT-7, 1995.*

[30] Goldstein, R. J. and Spores R. A., Turbulent Transport on the Endwall in the Region Between Adjacent Blades, *ASME Journal of Heat Transfer*, 1988, Vol. 110, pp. 257-268.

[31] Chung, J. T., and Simon, T. W., Three-Dimensional Flow Near the Blade Endwall Junction: Visualization in a Large-Scale Cascade Simulator, *ASME Paper 90-WA/HT-4, 1990.*

[32] Jabbari, M. J., Goldstein, R. J., Marston, K.C., and Eckert, R. G., Three-Dimensional Flow at the

Junction Between a Turbine Blade Endwall, *Warme-und Stoffubertragung*, 1992, Vol. 27, pp. 51-59.

[33] Khalatov, A. A., Improved Approach at an End Wall Heat Transfer Analysis: a Linear Vane and Curved Duct, *ASME Paper 98-GT-293*. The 1998 International Joint Power Generation Conference and Exposition, June 6-9, 1998, Stockhom, Sweden.

[34] Khalatov, A. A., Heat Transfer on Non-Porous and Porous Smooth End Wall of a Linear Guide Vane Model, *Heat Transfer 98, Proceedings of 11th IHTC*, Vol. 6, August 23-28, 1998, Kuongju, Korea.

[35] Khalatov, A. A., Shevtsov, S. V., & Syred, N. Heat Transfer Over Non-Porous and Porous Smooth End Wall of a Linear Guide Vane in the Presence of Freestream Turbulence, *ASME Paper 99-GT-329, 1999*.

[36] Hartland, J. C., Gregory-Smith, D. G., Harvey, N. W., & Rose M. G., Non-Axisymmetric End Wall Design: Part 2 Experimental Validation, *ASME Paper 99-GT-338, 1999*.

[37] Yan, J., Gregory-Smith, D. G., & Walker, P. J., Secondary Flow Reduction in a Nozzle Guide Vane Cascade by Non-Axisymmetric End-wall Profiling, *ASME Paper 99-GT-339*.

[38] Simon, T. W., Burd, S. W., Satterness, C. J., Kaszeta, R. W., & Oke, R. Documenting of Complex Flows in Gas Turbine Gas Path Cooling Systems, *Proc. Colloquium on Turbomachinery*, 1999. S. J. Song, Ed., pp. 1-16.

[39] Khalatov, A. A., & Lam, K. W. CFD Simulations on the Cyclone Cooling System of the Turbine Blade. Report of Cardiff University, No 1328, 1998, United Kingdom.

[40] Chyu, M. K., Ding, H. Heat Transfer in a Cooling Channel With Vortex Generators. Heat Transfer Gallery, Journal Heat Transfer, Transaction of ASME, Vol 119, 1997.

[41] Khalatov, A. A. & Syred N. Application of Swirl Flow Concept to Internal Blade Cooling. International Symposium on Heat Transfer in Gas Turbine Systems. 13 18 August, 2000, Izmir, Turkey. Book of Abstracts. International Centre for Heat and Mass Transfer, Ankara (IChHMT), Turkey.

[42] Goreloff, V., Goychenberg, M., & Malkoff, V. The Investigation of Heat Transfer in Cooled Blades of Gas Turbines. AIAA/SAE/ASME/ASEE, The 12th Joint Propulsion Conference, July 16-18, 2000, Orlando, Fl., USA. *AIAA Paper No 90-2144, 1990*.

[43] Bearman, P.W., & Harvey, J.K. Golf Ball Aerodynamics. Aeronaut, Vol. Q27, 1976, pp. 112-122.

[44] Azad, G., Huang, Y., & Han J.C. Impingement Heat Transfer on Dimpled Surfaces Using a Transient Liquid Crystal Technique. Journal of Thermophysics and Heat Transfer. Vol. 14, No 2, April-June 2000, pp. 186-193.

[45] Lake, J.P., King, P.J., & Rivir, R.B. Low Reynolds Number Loss Reduction on Turbine Blades with Dimples and V-grooves. The 38th

AIAA Aerospace Sciences Meeting and Exhibit, January 10-13 2000/ Reno, NV, USA. *AIAA Paper No 00-0738, 2000.*

[46] Chudnovsky, Ya.P., Kozlov, A.P., Shchukin, A.V., Agachev, R.S., & Gruzdev, V.N. Application of Vortex Generators for Combustion and Flame Stabilization. Izvestiya Akademii Nauk, Energetika, No 3, 1998, pp. 39-46 (in Russian).

[47] Shchukin, A.V., Kozlov, A.P., Chudnovsky, Ya.,P., & Agachev, R.S. Heat Transfer Enhancement by Spherical Dimples. Izvestiya Akademii Nauk, Energetika, No 3, 1998, pp. 47-64 (in Russian).

[48] Fiebig, M. Vortices, Generators and Heat Transfer. Proceedings of the 5th UK National Conference on Heat Transfer. Imperial College of Science and Technology, London, 17-18 September 1997, UK, pp. 1-39.

[49] Liou, T.M., Chen, C.C., & Tsai, T.W. Heat Transfer and Fluid Flow in a Square Duct with 12 Different Shaped Vortex Generators. *ASME Paper 99-GT-255, 1999.*

[50] Isaev, S.A. Modeling of organized vortex heat and mass transfer on dimpled curved surfaces: effects of natural convection, two-phase flow and combustion. Report of the S.Petersburg Academy of Civilian Aviation. 1999 (in Russian).

[51] Khalatov, A.A., Varganov, I.S., & Borisov, I.I. Blade with a Cyclone Cooling. Patent of Ukraine No 36360A, 08.12.99.

[52] Khalatov, A.A., Varganov, I.S., & Borisov, I.I. Cooled Blade of Gas Turbine. Patent of Ukraine No 32100A, 15.12.00.

[53] Khalatov, A.A., Varganov, I.S., & Borisov, I.I. Cooled Blade of Gas Turbine. Patent of Ukraine No 33785A, 15.02.01.